Simulation Analysis of Stability for Layered Soft Rock Underground Powerhouse Cavern Groups

Feng Zhang[1,a], Shuguang Zhou[1,b], Wenjun Wang[2,c*]

[1]Chongqing Panlong Pumped Storage Power Plant Co., Ltd. Chongqing, China
[2]College of Water Conservancy and Hydropower Engineering, Hohai University, Nanjing, China

[a]e-mail: 29868753@qq.com; [b]e-mail: 37565615@qq.com
* Corresponding author: [c]wenjunwang@hhu.edu.cn

Abstract. Currently, the construction of pumped storage power stations is in a peak period, and due to layout requirements at the station's location, it is sometimes challenging to find ideal geological conditions for the underground powerhouse location. This necessitates excavating underground caverns in areas with partially layered soft rock distribution. This study, based on the Panlong Pumped Storage Power Station project, delves deep into the stability of large underground cavern groups located in regions with partially layered soft rock distribution. The research reveals that significant deformations in the surrounding rock of the caverns with alternating soft and hard rock layers predominantly occur within the soft rock layers. Additionally, the larger principal stress concentrations tend to occur within the hard rock adjacent to the soft rock. The findings of this study have important practical implications for a comprehensive understanding of the displacement, stress, and plastic zone distribution patterns in such caverns' surrounding rock. These results can be used to guide the design of cavern support systems.

Keywords: Underground powerhouse; soft rock caverns; numerical simulation; stability analysis; panlong pumped storage power station

1 Introduction

Pumped storage power stations serve multiple functions such as peak shaving, valley filling, frequency regulation, phase adjustment, energy storage, and emergency backup. Currently, under the "dual carbon" goals, the construction of pumped storage power stations is progressing rapidly[1]. However, due to layout requirements at the station's location, it can sometimes be challenging to find an ideal construction site in areas where pumped storage power stations are needed. The geological conditions for the underground powerhouse are one of the major limiting factors. The span of underground powerhouses typically ranges from 25.0 to 30.0 meters, and stable excavation requires good

G. Zhao et al. (eds.), *Proceedings of the 2024 6th International Conference on Civil Architecture and Urban Engineering (ICCAUE 2024)*, Advances in Engineering Research 262,
https://doi.org/10.2991/978-94-6463-688-8_7

surrounding rock quality. In the past, caverns were constructed within high-strength hard rock. When there are partially soft rock sections around the cavern, the deformation and stress distribution in the surrounding rock become crucial factors in assessing the stability of the cavern[2]. Therefore, understanding the deformation and stress distribution patterns during excavation construction of partially soft rock underground caverns using numerical simulation techniques is of significant importance for stability analysis of underground cavern groups.

The academic and engineering communities have conducted extensive researches on underground powerhouses in hydropower stations. Ma et al.[3] performed three-dimensional elastoplastic finite element analysis on hard rock underground cavern groups in high-stress areas with a surrounding rock deformation modulus of 25.0 GPa, providing detailed insights into the displacement and stress field distribution after excavation. Dong et al.[4] analyzed the deformation characteristics during construction and the load on support systems for underground cavern groups with steeply inclined layered surrounding rock in the left bank powerhouse of the wudongde hydroelectric station. They studied the impact of rock structure and lithological differences on the deformation and relaxation of surrounding rock in giant caverns. Qian et al.[5] conducted excavation process simulations for underground cavern groups using a damage-based approach that considered weakening of cohesion and strengthening of friction angle in the surrounding rock. Huang et al.[6] analyzed the influence of geological and construction factors on displacement from the perspective of monitoring displacement and displacement rates, combined with geological data and excavation progress. Li et al.[7] combined the transversely isotropic elastic model with the jointed rock plastic model to study the deformation, stress changes, and plastic zone distribution during the excavation support process in shale regions. Yu et al.[8] compared and analyzed numerical simulation results under supported and unsupported conditions, investigating the influence of support on surrounding rock stress, displacement, and plastic zone distribution. Wu et al.[9] implemented construction techniques such as lower advance and self-advancing anchor rod pre-grouting, and prestressed anchor rod one-time grouting to control the depth of surrounding rock damage during the construction of high-stress underground caverns in houziyan. Zhou et al.[10] used micro-seismic monitoring for identifying and delineating damaged zones in the surrounding rock and for stability analysis during underground engineering construction. They also calibrated mechanical parameters during the dynamic rock damage process. In summary, recent research has mainly focused on underground caverns with relatively good rock properties and uniform surrounding rock quality. These studies have covered topics such as the deformation patterns of surrounding rock, stability analysis methods for cavern groups, construction simulation, damage mechanisms, and support measures. When considering the stability of underground factory chambers, the presence of layered soft rock geological conditions adds a significant layer of complexity. Soft rock often exhibits diverse and intricate mechanical properties and deformation behavior. These geological features can potentially lead to collapse, displacement, and deformation of underground chamber complexes, posing risks to both personnel safety and equipment integrity. Therefore, one of the key motivations behind this study is to gain a comprehensive understanding of the engineering behavior of soft rock, aiming to formulate effective support strategies and stability assessment methods.

Furthermore, with the continuous development of urbanization, the demand for underground spaces, including underground factories, warehouses, parking facilities, and more, is steadily increasing. Hence, addressing the stability issues of underground factory chambers constructed within layered soft rock becomes crucial for the sustainable development of urban infrastructure. Through this research, we can provide reliable guidance and design principles for future underground engineering projects to ensure that these underground structures can operate safely and remain stable over the long term within soft rock geological conditions. This paper, in the context of partially soft rock distribution in the underground powerhouse of the panlong pumped storage power station, utilizes nonlinear finite element analysis to investigate the impact of soft rock on the stability of cavern groups, providing technical support for similar engineering projects in the future.

2 Distribution of Soft Rock

Within the drilling depth range of the factory site, there are six layers of mudstone, silty mudstone, and siltstone distribution. The first layer is above the roof arch of the main factory building and has a thickness of approximately 3 meters. The second layer of soft rock has a thickness ranging from 4.70 meters to 5.60 meters and is distributed between elevations of 517.46 meters to 511.96 meters, with its bottom elevation approximately 5.4 meters higher than the design arch top excavation elevation of the factory building. The third layer of soft rock has a thickness ranging from 0.50 meters to 1.70 meters and is discontinuously distributed between elevations of 495.46 meters to 494.83 meters. The fourth layer of soft rock has a thickness ranging from 4.75 meters to 6.00 meters and is distributed on the upstream side of the main factory building between elevations of 486.69 meters to 480.69 meters. The fifth layer of soft rock is distributed near an elevation of 466.00 meters, penetrating the main transformer room. The sixth layer of soft rock is distributed at elevations below 454.00 meters to 460.00 meters, with a thickness of approximately 5 meters, mainly consisting of silty mudstone. The distribution of mudstone, silty mudstone, and other soft rocks in the underground factory is shown in Figure 1.

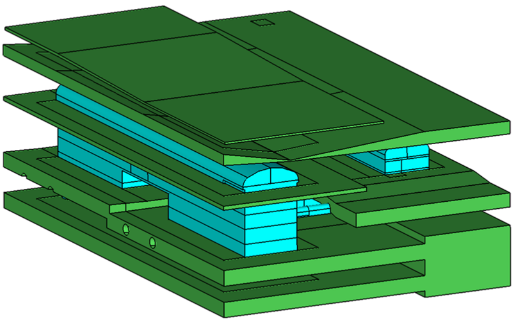

Fig. 1. Schematic diagram of soft rock distribution in longitudinal section of the generating unit

3 Calculation Model and Parameters

3.1 Finite Element Analysis (FEA) Model

The three-dimensional finite element mesh modeling scope of the underground powerhouse of the Panlong pumped storage power station is as follows: the axial direction of the powerhouse is taken as 669m; the left side of the model is located 250m away from the left wall of the main powerhouse, while the right side is located 250m away from the right wall of the main powerhouse. The unit section is a total of 169m; the upstream is located 250m away from the upstream wall of the main powerhouse, while the downstream is located 200m away from the downstream wall of the main transformer chamber. In the vertical direction, below the bottom of the main powerhouse, the scope extends 200m downwards, while upwards, it extends from the top of the main powerhouse arch to the ground surface. The X-axis represents the axial direction of the main powerhouse, with positive values directed towards the secondary powerhouse. The Y-axis is perpendicular to the axial direction of the main powerhouse, with positive values directed towards the main transformer chamber. The Z-axis represents the vertical direction, with positive values pointing upwards. The excavation portion of the mesh can be seen in Figure 2.

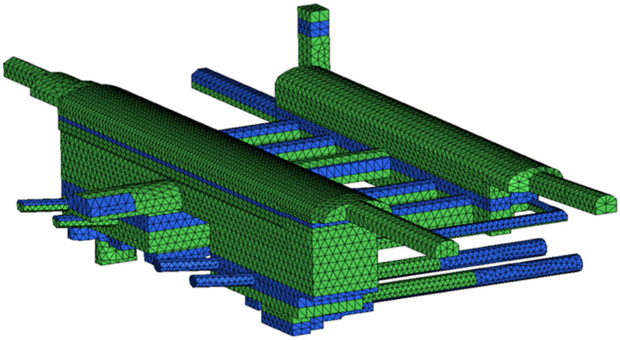

Fig. 2. Computational mesh for the excavation portion of the powerhouse area

3.2 Initial Stress Field

Based on the measured ground stress data in the power station's facility area, a multiple linear regression analysis was conducted using the least squares method to infer the initial stress field within the computational region. The results indicate the following characteristics of the stress distribution: Along the powerhouse axis direction, the stress σ_X ranges from -5.06 MPa to -6.15 MPa. In the direction perpendicular to the powerhouse axis, the stress σ_Y ranges from -3.86 MPa to -4.88 MPa. In the vertical direction, the stress σ_Z ranges from -5.05 MPa to -7.86 MPa. The values of stress components all exhibit a distribution pattern of increasing with decreasing elevation.

3.3 Excavation Sequence

The numerical simulation models the actual excavation and construction process of underground caverns, followed by the implementation of rock bolting and anchoring support after excavation. By realistically simulating the construction process of the underground powerhouse, you can observe the displacement patterns of the surrounding rock of the high side walls during excavation. The layout and layered excavation sequence schematic diagram of the powerhouse cavern group can be seen in Figure 3.

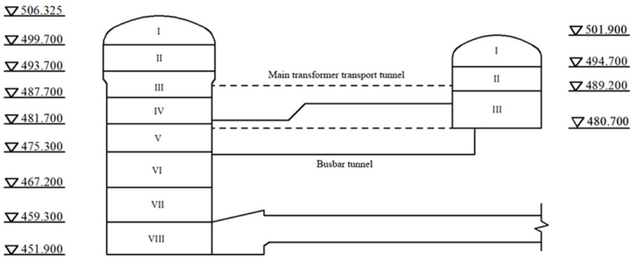

Fig. 3. The schematic diagram of the layout and layered excavation of the underground powerhouse cavern group in the panlong pumped storage power station

3.4 Rock Support

The main factory building support measures include: 20cm fiber reinforced concrete spraying for the roof arch; 100kN prestressed anchor bolt Φ32/28@1.125m×1.5, arranged in a diamond pattern with a length of 9m/6m; T=2000kN prestressed anchor cables, length ranging from 28-35m, arranged in 8 rows with a spacing of 4.5m. Below the bus layer, 20cm fiber reinforced concrete spraying is done for the side wall; 100kN prestressed anchor bolt Φ32/28@1.2m×1.2, arranged in a diamond pattern with a length of 6m/9m; upstream there are 5 rows and downstream there are 4 rows of T=1200~2000kN prestressed anchor cables, with a length ranging from 28-35m and a spacing of 4.5~5.0m.

3.5 Computational Model

The study uses the Mohr-Coulomb elastoplastic model for three-dimensional nonlinear finite element analysis of cavern groups. The model assumes that the rock mass primarily undergoes elastic deformation before reaching the strength limit and is determined by two elastic deformation parameters (E,ν or K,G). When the stress exceeds the conditions for shear failure in the rock mass, plastic yielding is assumed to occur, determined by the strength parameter c,ϕ . Plastic strains are calculated following the principles of plastic flow in plastic mechanics. Since plastic strains determined by the orthotropic (associated) flow rule often overestimate the plastic volume strain (overestimate shear dilatancy), a non-orthotropic (non-associated) flow rule is generally used.

This requires introducing a shear dilation angle parameter ψ , which is different from the internal friction angle ϕ. Typically, the shear dilation angle ψ is much smaller than the friction angle, and it is usually taken as $10^{\circ}\sim 20^{\circ}$.

3.6 Calculation Parameters

According to the design, the geological parameters for the surrounding rock of the Panlong Pumped Storage Power Station underground chamber group can be found in Table 1, and the mechanical parameters for the support materials can be found in Table 2.

4 Calculation results

4.1 Cavern Perimeter Deformation Patterns

Figures 4 to 9 provide contour plots of the deformation patterns in three directions around the underground powerhouse after the completion of excavation. The overall deformation of the cavern exhibits a contraction state, with deformation occurring in the direction perpendicular to the open face around the chambers. The largest axial deformations primarily occur in the side walls of the main powerhouse's end walls and the installation bay, with a maximum horizontal displacement of 24.23mm. The top arch has subsided vertically, with significant deformation in the middle, and the bottom slab has rebounded. The maximum displacement of the top arch after excavation is 32.25mm. In the upstream wall of the main powerhouse, the displacement along the vertical axis points downstream, with relatively large displacement values in the central portion. The maximum horizontal displacement is 50.18mm. In the downstream wall, the maximum horizontal displacement is mainly located within the rock mass between the main bus chambers, pointing upstream. The largest horizontal displacement in this area is 36.07mm. From Figures 5 and 9, it can be observed that the maximum horizontal displacements (in the axial and water flow directions) around the cavern occur in the soft rock layer 6, indicating the significant influence of soft rock on cavern deformations.

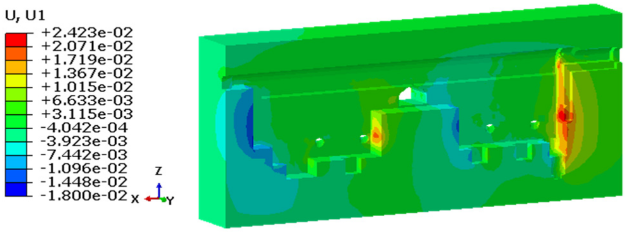

Fig. 4. Displacement distribution cloud map in the upstream axial direction of the underground factory building (m)

Table 1. Recommended values of physical and mechanical parameters of cavern surrounding rock

Rock Type	**Rock Description**	$\rho(kg/m^3)$	E(GPa)	ν	c(MPa)	$\varphi(^\circ)$
Class III	Fine-grained and medium to coarse-grained sandstone	2550	7~8	0.23	0.9~1.0	45~47.7
Class IV	Conglomerate and siltstone	2500	4~5	0.26	0.3~0.4	31~35
Class V	Mudstone	2300	0.5~0.7	0.30	0.1~0.15	19.3~24.2

Table 2. Recommended values for mechanical parameters of supporting materials

Support Type	**Description**	**Density /kg·m^{-3}**	**Young's Modulus /GPa**	**Poisson's Ratio/μ**
Concrete Lining	Steel Fiber-Reinforced Concrete (CF30)	2 500	30	0.20
	Standard Concrete (C25)		28	
Ordinary Anchor Bars	Cement Mortar Anchor Bars (HRB400)	7 850	200	0.27

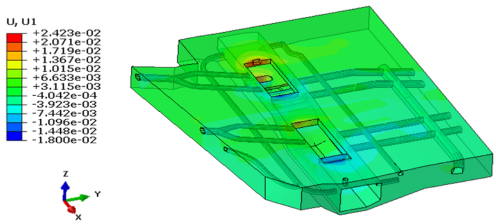

Fig. 5. Displacement distribution cloud map in the direction of the 6-axis line in soft rock (m)

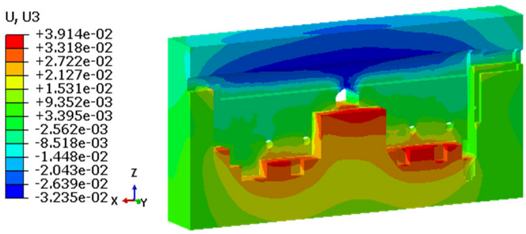

Fig. 6. Displacement distribution cloud map in the upstream vertical direction of the underground factory building (m)

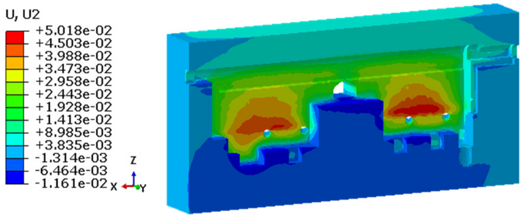

Fig. 7. Displacement distribution cloud map of water flow direction in the upstream of the underground factory building (m)

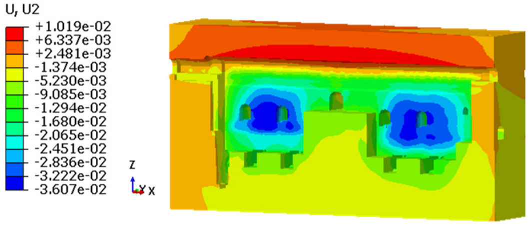

Fig. 8. Displacement distribution cloud map of water flow direction in the downstream of the underground factory building (m)

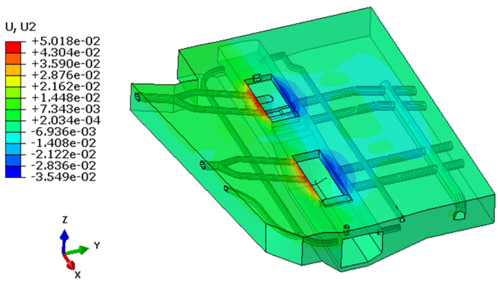

Fig. 9. Displacement distribution cloud map of water flow direction in the soft rock layer 6 (m)

4.2 Cavern Perimeter Stress Distribution

From Figure 10, it can be observed that after the excavation of the main powerhouse, the significant principal compressive stresses around the cavern are mainly distributed at the arch shoulders of the entrance tunnel, the arch shoulders of the main powerhouse's supply fan room and exhaust fan room, the corners of the side walls, the bottom slab, the corners of the side walls and the bottom slab. The maximum principal compressive stress value is -34.12 MPa. From Figures 11 and 12, it can be seen that the principal compressive stress values in the soft rock are relatively small, with the maximum principal compressive stress occurring near the corner of the entrance tunnel adjacent to soft rock layer 3. The magnitude of the principal tensile stresses around the cavern is small and mainly distributed in the Class III surrounding rock between soft rock 3 and soft rock 6, the end walls of the main powerhouse, and the central part of the bottom slab in the installation chamber. The distribution of tensile stresses in soft rock 3 and soft rock 6 is very limited, and their values are much smaller than those in the hard rock.

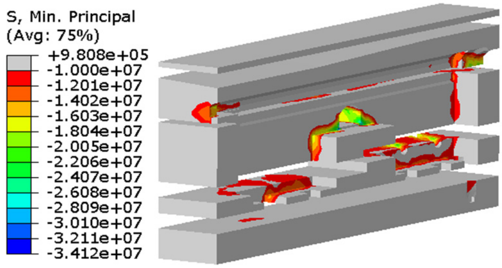

Fig. 10. Cloud map of principal compressive stress distribution in hard rock on the upstream side of the main powerhouse (Pa)

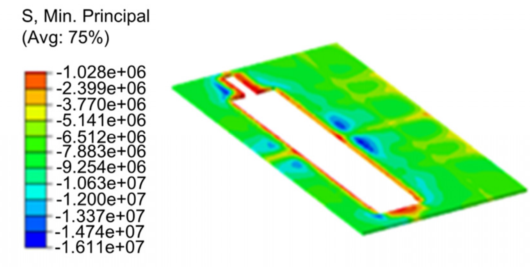

Fig. 11. Cloud map of the distribution of principal stresses on soft rock layer 3 (Pa)

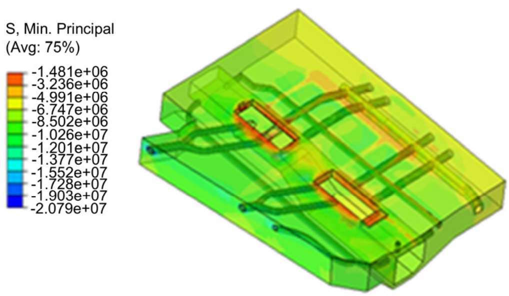

Fig. 12. Cloud map of the distribution of principal stresses on soft rock layer 6 (Pa)

4.3 Surrounding Rock Plastic Zone

After the excavation is completed, the plastic zones in the soft rock caverns are relatively extensive. Figure 13 provides the contour map of the plastic zone distribution in soft rock layer 3, and Figure 14 provides the contour map of the plastic zone distribution in soft rock layer 6. Upon completion of the excavation of the second level of the main powerhouse, the soft rock layer 3 that passes through the main powerhouse is also excavated, and the plastic zone gradually expands with the progress of excavation. After excavation is completed, the plastic zone in the soft rock extends from the face towards the interior. The extension depth of the plastic zone in the upstream wall-side soft rock is approximately 4.5 meters, while in the downstream wall-side soft rock, it is about 4 meters. In the upstream side of the main powerhouse, the plastic zone in soft rock layer 6 is relatively extensive, with a maximum extension depth of up to 12 meters in the direction perpendicular to the powerhouse axis. In the downstream side of the main powerhouse in soft rock layer 6, the plastic zone extends up to a maximum depth of about 6.5 meters in the direction perpendicular to the powerhouse axis.

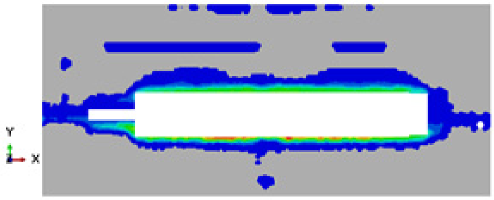

Fig. 13. Cloud map of plastic zone of soft rock 3 after excavation

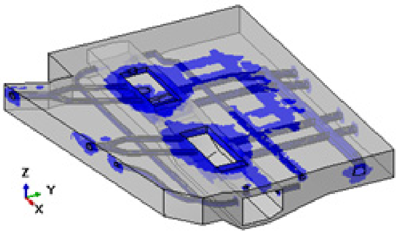

Fig. 14. Cloud map of plastic zone of soft rock 6 after excavation

5 Conclusions

This paper, based on the panlong pumped storage power station as the engineering context, utilizes nonlinear finite element analysis to simulate the excavation process of caverns, taking into account the varying distribution of soft rock in the powerhouse area. From the computational results, it is evident that the horizontally layered distribution of soft rock has a significant impact on cavern deformation and stress. In contrast to the relatively smooth deformation curves of homogeneous surrounding rock, the presence of horizontally layered soft rock causes noticeable deviations. Substantial horizontal deformation of the caverns mainly occurs in thicker layers of soft rock. The stress values in soft rock are considerably lower than those in hard rock. Significant compressive stresses around the caverns are primarily concentrated in the hard rock adjacent to the soft rock. In particular, corners and junctions where soft rock meets hard rock, such as the arch shoulders of entrance tunnels, the supply fan room of the main powerhouse, the arch shoulders of the exhaust fan room, and the corners of the side walls and bottom slab, are more susceptible to stress concentration. The plastic zone in soft rock is larger than that in hard rock, and the depth of the plastic zone increases with the thickness of the soft rock layer. Therefore, reinforcement measures should be implemented for the thicker layers of soft rock.

References

1. Yang, R.P., Fan, Z.T. (2023) Application and Prospects of Pumped-storage Power Stations in New Power System.Sino-Global Energy, 28:12-27.
2. Zheng, D.X., Su, C. (2018) Optimization Analysis of Excavation Schemes for Large Underground Caverns under Soft Rock Geological Conditions. Water Power, 44:61-64.
3. Ma, X.D. (2016) Surrounding Rock Stability Evaluation of Large Span Cavern Group with High Stress of Guandi Hydropower Station. Chinese Journal of Underground Space and Engineering, 12:564-570.
4. Dong, Z.H., Niu, X.Q., Ding, X.L., Weng, Y.H., Huang, S.L., Pei, Q., Zhang, L. (2018) Deformation Characteristics and Feedback Analysis of Surrounding Rock of Underground Powerhouse at Left Bank of Wudongde Hydropower Station. Rock and Soil Mechanics, 39:326-336.
5. Qian, M.M.，Leng, X.L., Wang, C.,Li, H.L., Li, G. (2021) Effects of a Damage-based CWFS Model on Rock Mass Stability in Large Underground Caverns. Science Technology and Engineering, 21:3763-3769.
6. Huang, Q.X., Deng, J.H., Su, P.Y., Wang, Q.J., Y. P. (2011) Displacement Characteristics Analysis of Surrounding Rock in Underground Powerhouse Chambers at Pubugou Hydropower Station During Construction. Chinese Journal of Rock Mechanics and Engineering, 30: 3032-3042.
7. Li,W.J., Ren, X.H., Zhang, J.X., Wei, P. (2022) Study on Surrounding Rock Stability of Underground Powerhouse Cavern Gropup in Slate Area. Water Power, 48:74-79.
8. Yu, X.P., Liu, Q.Y. (2018) Simulation Analysis of Surrounding Rock Support for a Large Underground Cavern Group of a Hydropower Station. Water Resources and Power, 36:97-100.
9. Wu, Y., Li, D., Luo, D.Z., Wang, J., Li, H.T., Yao, Q. (2021) Control Technology of Loosing Surrounding Rock and Damage of Underground Cavern Group in Houziyan Hydropower Station. Water Resources and Power, 39:142-145.
10. Zhou, C., Yin, J.M., Zhou, C.H., Wang, Y., Xu, C.M. (2020) Stability Analysis of Surrounding Rock Mass of Underground Caverns at Huanggou Hydropower Station Considering Cumulative Microseismic Damage Effect. Chinese Journal of Rock Mechanics and Engineering, 39:1011-1022.